Springer

KSME

Journal of Mechanical Science and Technology 26 (5) (2012) 1591~1597
www.springerlink.com/content/1738-494x
DOI 10.1007/s12206-012-0305-y

Single discharge thermo-electrical modeling of micromachining mechanism in electric discharge machining †

Yasin Sarikavak[1,*] and Can Cogun[2]

[1]*Railway Research and Technology Center, Turkish State Railways, Behicbey, Ankara, 06105, Turkey*
[2]*Mechanical Engineering Department, Middle East Technical University, Ankara, 06800, Turkey*

(Manuscript Received May 17, 2011; Revised December 5, 2011; Accepted January 25, 2012)

Abstract

In this study, single discharge thermo-electrical model of workpiece material removal in electrical discharge machining (EDM) was developed. Developed model includes generation of energy in liquid media, variation of plasma channel radius and transfer of heat from the channel by the electrical discharge. Effect of generated energy in plasma channel on workpiece removal was theoretically investigated by using different experimental parameters used in literature. The developed model finds the temperature distribution in the workpiece material using finite element solver ANSYS Workbench (v.11) software. It's assumed that the workpiece material reaches the melting point of workpiece material was removed from the surface. Electrical discharge process was simulated by using transient thermal analysis. The developed model has also been validated by comparing the theoretically obtained material removal values with the experimental ones.

Keywords: Electric discharge machining (EDM); Finite element analysis; Material removal rate; Molten radius; Plasma channel radius; Thermal model

1. Introduction

Electric discharge machining (EDM) is a nontraditional manufacturing process used for manufacturing complex shaped molds, tools and components. Process depends on the electrical discharge between electrode and workpiece that erodes small volume on workpiece [1].

Generally, the machining mechanism was modeled by a thermal model for one electrical discharge. DiBitonto et al. [2] used a point heat source model for presenting the spark on workpiece surface. The developed point heat source model uses the discharge power as boundary condition instead of temperature between plasma and workpiece. In their analysis, constant ratio of applied power is assumed to reach to workpiece surface. The calculated theoretical results (R_P) are validated by the experimental data. In Patel et al. [3] work, the discharge power of the plasma is used as heat source between plasma and anode interface. Cylindrical plasma with variable mass model is developed by Eubank et al. [4] for sparks created by electrical discharge in liquid media. Numerical solution of the model provides plasma radius (R_P) and temperature as a function of pulse time for fixed current, electrode gap and power fraction remaining in the plasma. Plasma temperature varies between 2000°C and 60000°C under 0-100 kg_f/mm^2 pressure for different experimental parameters. Marafona and Chousal [5] used a finite element solver ABAQUS/standard for modeling EDM process. They used DiBitonto's [2-4] experimental results to validate their model. The forced heat convection caused by fluid flowing through the mesh is not considered. In Kansal's study [6], an axisymmetric two-dimensional model for powder mixed dielectric has been developed using finite element method. The developed model calculates first the temperature distribution in the workpiece material using ANSYS software and then the material removal rate is estimated from the temperature profiles. The radius of the spark for powder mixed dielectric liquid is taken 30-50% larger than the classical EDM process. Theoretical findings are found compatible with the performed experimental results. Das et al. [7] developed a finite element model for a single spark by using discharge power as boundary condition at workpiece plasma interface. In their study, DEFORM software was used to solve transient temperature distribution problem. Yadav et al. [8] investigated the thermal strains appear after the sparks on the workpiece surface. Van Dijck and Snoeys [9] also investigated workpiece temperature distribution in EDM by using a transient thermal model on workpiece surface. Salah's work [10] presents the numerical results concerning the temperature distribution in EDM process. Kumar

*Corresponding author. Tel.: +90 312 211 10 41 Ext: 8483, Fax.: +90 312 211 07 35
E-mail address: yasinsarikavak@tcdd.gov.tr
† Recommended by Associate Editor Vikas Tomar.

[11] investigated the thermal strains and micro cracks on workpiece surface by using heat transfer by conduction. Heat losses by radiation and other forms are neglected. The energy received by the workpiece is assumed to be 17 to 20% of the discharge channel energy. Some experimental findings are compared with the theoretical ones and closer results are observed. In Ghosh's study [12], it is concluded that electrostatic forces formed during small pulse times (< 100 μs) are dominant on surface strain distribution on metallic surfaces. In Allen and Chen study [13], thermal strains formed after the cooling process is investigated by using two-dimensional model. Molybdenum was used as workpiece and it is assumed that material that reaches the melting point is removed from the surface. Experimental results are found consistent with theoretical results.

(i) In published studies, a point heat source model for presenting the spark on workpiece surface is assumed and experimantations are performed to validate the point model in EDM field. However, the Gaussian heat input model is a well known and well accepted heat input model that has been used successfully in modelling of gas-metal arc welding processes where transient heating from a heat source is involved. So, the use of Gaussian distribution in modelling plasma channel temperature in EDM would be a much proper approach.

(ii) In most of the published single spark thermo-mathematical modeling studies, the authors performed limited number of experiments to verify their theoretical findings. The experimental findings of the other researchers, performed at different machining conditions, should be used for better comparison and stronger verification of the theoretical findings.

(iii) In most of the published studies only the plasma temperature or plasma power is input to the model to calculate the plasma radius. For better understanding of single spark discharge behavior, effects of temperature and power input on the plasma radius must be considered independently and compared carefully.

In this study, four different temperature and plasma power values for the plasma channel are used. Effects of machining parameters, namely pulse time (t_d), pause time (δ), discharge current and discharge values, on workpiece material removal are theoretically investigated. Theoretical findings obtained from the proposed model are validated by three different experimental works published [1, 2, 6]. In this study, Gaussian type heat source distribution is used in modeling of spark and convection heat transfer between workpiece and dielectric liquid is introduced in modeling studies.

2. Modeling of spark formation in EDM

2.1 Mathematical modeling

2.1.1 Assumptions

In this study, due to the complex nature of EDM material removal process the following assumptions are made to solve the proposed model mathematically:

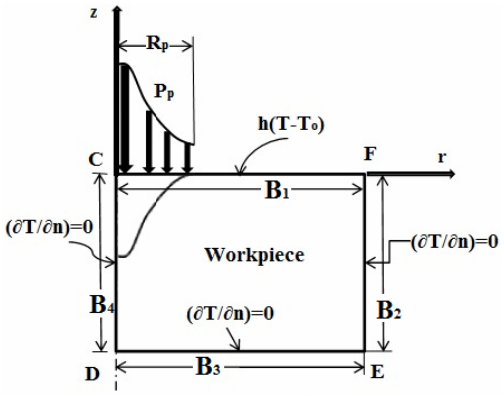

Fig. 1. Heat transfer model for a spark in EDM [6, 8].

(i) The model is developed for a single spark.
(ii) The workpiece is homogeneous and isotropic.
(iii) The heat transfer to the workpiece is by conduction.
(iv) Spark forms a circular heat source on workpiece.
(v) Plasma channel has a uniform cylindrical shape.
(vi) The domain is considered axisymmetric.
(vii) Heat loss due to radiation is neglected.
(viii) The heat source distribution is Gaussian type.

2.1.2 Thermal model

Plasma channel occurs at the interface between tool and workpiece. High temperature due to electrical current in plasma channel causes material removal on workpiece surface during pulse time. Pulse time, plasma power and plasma channel radius have primary effect on crater formation [14]. Initial studies in the literature use a point heat source model [2-4, 15]. It is clear from the literature that defining a plasma channel radius varies with discharge current and pulse time on workpiece surface gives more realistic results than the point heat source model. Due to this reason, varying plasma channel radius with process parameters approach is used in this study.

Conduction heat transfer model for an axisymmetric solid surface is expressed as follows:

$$\rho C_P \frac{\partial T}{\partial t} = \left[\frac{1}{r}\frac{\partial}{\partial r}\left(\kappa r \frac{\partial T}{\partial r} \right) + \frac{\partial}{\partial z}\left(\kappa \frac{\partial T}{\partial z} \right) \right]. \quad (1)$$

Here, ρ is density, C_p is heat capacity, κ is thermal conduction coefficient, T is temperature, t is time, r and z are coordinate axes.

Model is symmetric around z-axis (Fig. 1). Due to existence of dielectric liquid outside of the plasma channel surface, there is convection heat transfer. Boundary conditions are,
until R_P:

$$(\kappa\, \partial T/\partial z) = P_p \quad \text{or} \quad (\kappa\, \partial T/\partial z) = T_p; \quad (2)$$

outside of the R_P:

$$\kappa \frac{\partial T}{\partial z} = h(T - T_0)\ ; \quad (3)$$

Table 1. Experimental parameters [1].

Exp. No	I_d (A)	δ (μs)	t_d (μs)	R_p (μm)	P_p (W)
E1	3	50	50	18.295	180
E2	6	50	50	24.648	330
E3	12	50	12	17.722	540
E4	12	50	25	24.477	540
E5	12	50	50	33.206	540
E6	12	50	100	45.048	540
E7	25	50	50	45.529	1075

for B_2, B_3 and B_4 boundaries:

$$(\partial T/\partial n) = 0. \quad (4)$$

Here, h is the heat transfer coefficient between dielectric liquid and workpiece, T_o is the initial temperature (equal to room temperature), T is the temperature value, n is the normal of surface, P_P is the plasma power and T_P is the plasma temperature [6, 16].

2.1.3 Energy formation and plasma temperature

The total P_p is the product of the current flowing (I_d) and the discharge voltage difference between the electrodes (U) during the plasma discharge [7, 9, 17, 18]. A portion of P_P is conducted away by the cathode, a portion is conducted away by the anode and the remaining portion is dissipated in to the dielectric [2, 3]. A constant temperature is assumed on workpiece surface during pulse time [19, 20]. The maximum temperature at the center of the plasma channel reaches above the melting temperature of the material. For energy densities of 3 J/mm^3, a local plasma temperature is as high as 40000°C [2]. Kansal's study [6] suggests 3000-6000°C temperature values at the center of the plasma channel. This value varies in accordance with the used machining parameters and the ratio of total plasma power reaches the workpiece. Other studies specify plasma channel temperatures between 8000°C and 20000°C [21, 22].

In this study, both T_p (3000°C, 5000°C, 8000°C and 10000°C) and P_P are used in calculation of workpiece temperature distribution and material removal rate.

2.1.4 Plasma radius

Researchers derived various empirical equations for determining plasma radius (R_P). In this study, the equation introduced by Ikai and Hashiguchi [23], which express the plasma radius in terms of I_d and t_d (Eq. (5)), is used to calculate R_P.

$$R_p = (2.04\times10^{-3})\,(I_d^{0,43})\,(t_d^{0,44}) \quad (5)$$

3. Experimental studies

In this study, the experimental results of three published studies [1, 2, 6] are used to check the validity of the developed model. Ozgedik and Cogun [1] used SAE 1040 steel as workpiece material and kerosene as dielectric liquid. The experimental parameters and properties of workpiece used in the study are shown in Table 1 and 2. Table 3 shows experimental parameters and calculated plasma radius for DiBitonto et al. study [2] in which steel workpiece and kerosene dielectric liquid are used. In Ref. [6], AISI D2 mold steel is used as workpiece (Table 4) and kerosene as dielectric liquid. The used experimental parameters are shown in Table 5.

In this study, convection heat transfer coefficient between steel and dielectric liquid (kerosene) is taken as 10000 W/m^{2}K [8]. Plasma channel consist of vaporized liquid with $\kappa = 0.06$ W/mmK, $\rho = 1.5\times10^{-36}$ kg/mm^3 and C_p=15000 J/kgK [5].

Table 2. Physical properties of steel workpiece material [1].

Melting temperature (T_m) (°C)	1535
Thermal conductivity (κ) (W/mK)	56.1
Specific heat (C_p) (J/kgK)	575
Density (ρ) (kg/m^3)	7545

Table 3. Experimental parameters [2].

Exp. No	I_d (A)	U (V)	δ (μs)	t_d (μs)	R_p (μm)
E1	2.34	25	1	5.6	6.27
E2	2.85	25	1.3	7.5	7.77
E3	3.67	25	2.4	13	11.02
E4	5.3	25	2.4	18	14.90
E5	8.5	25	2.4	24	20.72
E6	10	25	2.4	32	25.22
E7	12.8	25	3.2	42	31.61
E8	20	25	3.2	56	43.47
E9	25	25	4.2	100	61.76
E10	36	25	4.2	180	93.57
E11	44	25	5.6	240	115.77
E12	58	25	7.5	420	166.77
E13	68	25	10	560	202.68

Table 4. Thermal and physical properties of AISI D2 mold steel [2].

Melting temperature (T_m) (°C)			1710
Density (ρ) [kg / m^3]			7700
Temp.(K)	Thermal conductivity (κ) [W/m°C]	Thermal Expansion Coef. [/°C] (×10^{-6})	Specific heat (Cp) [J/kgK]
298	29.0	5.71	412.21
673	29.5	6.90	418.36
1100	30.7	10.2	421.83
1990	32.3	12.0	431.00

Table 5. Experimental parameters [6].

Exp. No	I_d (A)	U (V)	δ (μs)	t_d (μs)	R_p (μm)
E1	3.2	30	100	100	25.51
E2	6.5	30	100	100	34.60
E3	12	30	100	100	45.04
E4	6.5	30	100	100	34.60
E5	6.5	30	100	200	46.95
E6	6.5	30	100	300	56.11
E7	6.5	30	50	100	34.60
E8	6.5	30	100	100	34.60
E9	6.5	30	200	100	34.60
E10	6.5	30	300	100	34.60

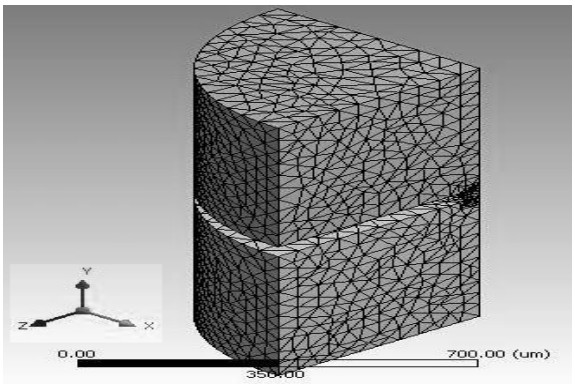

Fig. 2. 3-D view of the tetrahedron meshed model.

4. Modeling and analysis

2-D sketch of the system (workpiece and tool) is drawn by using Design Modeler of ANSYS (Geometry Module) and the 3-D model is formed after dimensioning. Reasons for using 3-D model are: a) use of electrically conductive composite materials (3-D structural deformation case), b) use of very small and non-cylindrical workpieces in recent EDM studies.

The simulation module is started after forming the model. In this study, time dependent (transient) thermal analysis type is selected. Thermal material properties of the workpiece, plasma channel and tool were entered to the simulation module of the model. In FE calculations, tetrahedron shape element is used for meshing workpiece and tool electrodes (Fig. 2). Tetrahedron meshing with 0.05 mm element size provides closer results to the experimental findings than the hexagonal element meshing. Element size is taken as 0.009 mm for the contact points between plasma channel and the electrodes to obtain accurate results. Three-dimensional model consists of 16960 nodes and 9870 elements.

After meshing, boundary conditions are entered to the model. During pulse time, P_p or T_p is applied to the plasma channel. Convection heat transfer is defined on outer surfaces of the plasma channel and workpiece in contact with dielectric liquid. Temperature distribution at the end of the plasma is Gaussian type. The program forms the mathematical model and generates the solution (the workpiece temperature distribution at the end of pulse time) in accordance with the defined element type, initial conditions and boundary conditions.

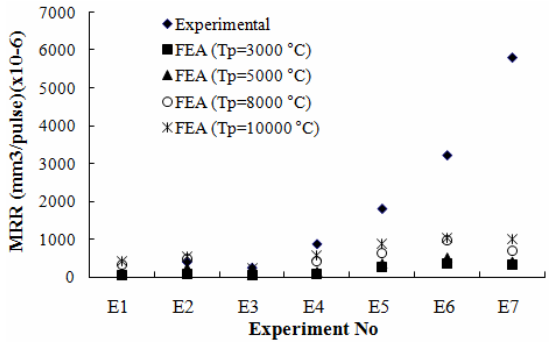

Fig. 3. Experimental [1] and FEA MRR results (T_P input to FEA).

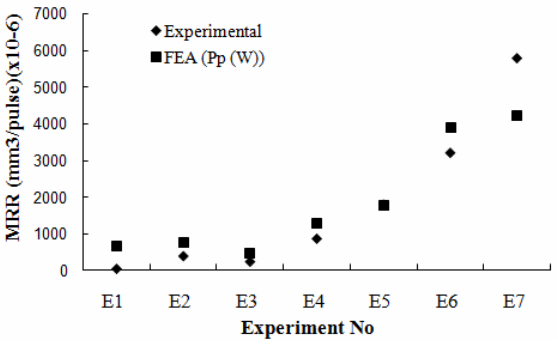

Fig. 4. Experimental [1] and FEA MRR results (P_P input to FEA).

5. Results and discussion

5.1 Comparison of the FEA results with Ref. [1]

For T_p = 10000°C, molten volume of workpiece is calculated as 251×10^{-6} mm^3/pulse. The experimental value is nearly equal to this value (254×10^{-6} mm^3/pulse). Theoretically T_P reaches to 110000°C at the center of the plasma channel for 540 W P_p input. Both analyses indicate that temperature values decrease when moving radially outward from the center of the channel. The temperature distribution obtained from FEA is in agreement with the assumed Gaussian distribution. Workpiece temperature is increased to boiling temperature of the material. Molten workpiece material volume for 540 W P_p input is 1770×10^{-6} mm^3/pulse. The experimental value is also very close to this value (1811×10^{-6} mm^3/pulse).

Figs. 3 and 4 show comparison of FEA and Ref. [1] experimental results. The FEA results obtained by P_P input to the model show that the maximum temperature is above 60000°C. Fig. 3 shows that FEA and experimental MRR results for 3000°C-10000°C (at 12 A I_d values) plasma channel temperature are very consistent for E1-E5 experiments. However, FEA results are lower than the experimental ones for E6 and

E7 data points (experiments). This indicates that the assumption of constant temperature in the plasma channel during pulse duration for high energy discharge pulses is not a proper approach. From Fig. 4, it is clear that the MRR values obtained from FEA and experiments are close for P_P input to the plasma channel. So, it is found that P_P input to the model is much better approach than entering T_P values.

5.2 Comparison of the FEA results with Ref. [2]

Melt radius (R_m) obtained from FEA is 25 μm for experimental settings of E5 (Table 1) at T_p= 3000°C. The experimental finding of R_m for the same machining settings is 24 μm. E8 FEA results shows that plasma temperature reaches 79000°C at the center of the plasma channel for P_p = 500 W. R_m calculated and experimentally found for this setting are 91 μm and 38 μm, respectively.

As shown in Figs. 5-8, theoretical (FEA) and experimental R_m for varying I_d and t_d values are consistent at I_d lower than 20 A and t_d shorter than 100 μs. Figures show that small amount of material is removed (i.e. small R_m) from workpiece at low I_d and t_d values. Increasing I_d and t_d settings result in increasing difference between theoretical and experimental R_m values. In FEA stage of this study, the workpiece material reaches the melting point is assumed to be removed from the workpiece surface. However, it is known that a portion of the molten metal resolidifies on the workpiece surface. The difference between the molten metal and removed from the crater is higher especially for high energy (high I_d and t_d values) pulses [10]. In high energy pulses, larger proportion pulse energy is spent for melting craters (with large radius) which are resolidified under the cooling effect of larger radius dielectric columns when the plasma channel dies [24].

5.3 Comparison of the FEA results with Ref. [6]

Theoretically calculated R_m value is 53 μm for experimental settings of E4 at T_p = 5000°C. The experimental finding (58 μm) is consistent with this value.

Also, very consistent R_m results are obtained (FEA 80 μm and experimentally 75 μm) for E6 (at T_p = 5000°C). FEA results indicate that at the same machining settings R_m is 53 μm for t_d = 100 μs and 80 μm for t_d = 300 μs. The results indicate that pulse time increases significantly R_m values.

Experimental and theoretical R_m results are close especially for small I_d at T_p = 3000°C (Fig. 9). With increasing I_d, theoretical R_m values are getting smaller than the experimental ones. Theoretical and experimental R_m values are very close at T_p = 5000 °C and I_d = 6 A. Theoretical R_m values are not consistent with experimental ones for T_p = 10000°C and small I_d values. R_m values are getting closer for higher I_d values (up to 10 A). In the FE analysis in which P_p is input to the model (Fig. 10), theoretical findings are higher than the experimental ones. From the figure it is clear that R_m increases with increasing I_d for experimental and theoretical cases.

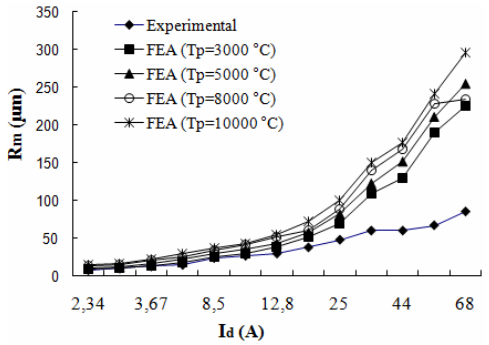

Fig. 5. Experimental [2] and FEA R_m results (T_p input to FEA).

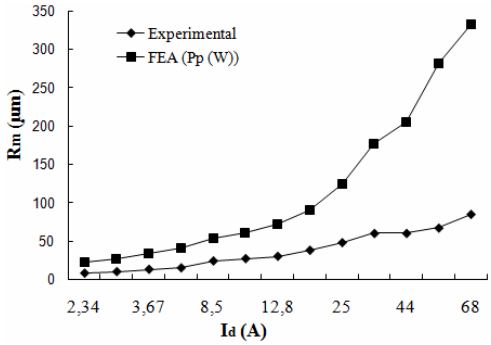

Fig. 6. Experimental [2] and FEA R_m results (P_p input to FEA).

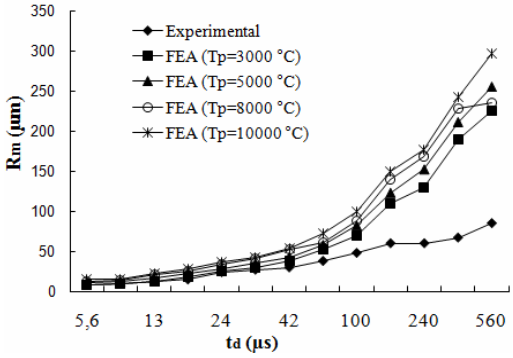

Fig. 7. Experimental [2] and FEA R_m results (T_p input to FEA).

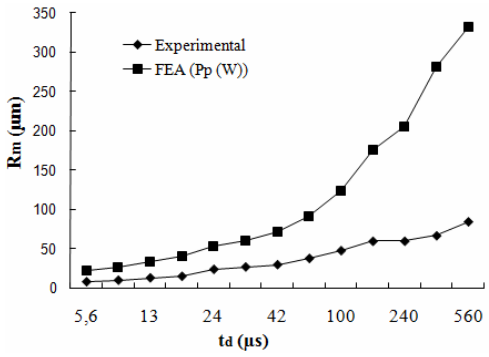

Fig. 8. Experimental [2] and FEA R_m results (P_p input to FEA).

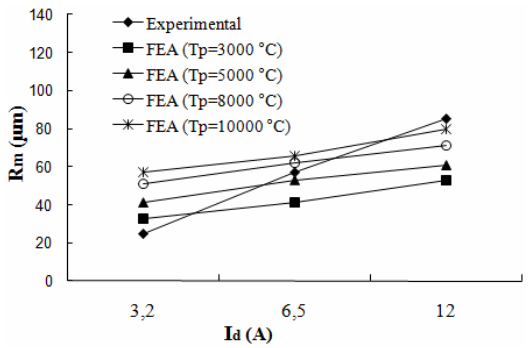

Fig. 9. Experimental [6] and FEA R_m results (T_p input to FEA).

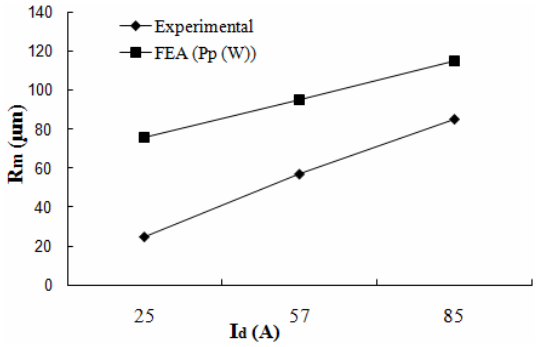

Fig. 10. Experimental [6] and FEA R_m results (P_p input to FEA).

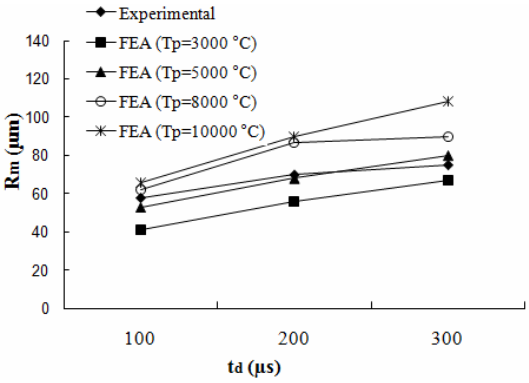

Fig. 11. Experimental [6] and FEA R_m results (T_p input to FEA).

Experimental and FEA R_m values for varying t_d by using T_P input to the model are shown in Fig. 11. At T_p = 5000°C, theoretical R_m values are close to the experimental ones. For T_P 10000°C (Fig. 11) or power input (Fig. 12) cases, the theoretical R_m values are 35-50% higher than the experimental ones (due to reason explained in the last paragraph of section 5.2).

6. Conclusion

In this study, a 3-D transient thermal model for a single discharge was developed to calculate the molten metal radius (R_m) and material removal rate (MRR) in EDM process. Developed model includes several primary aspects of EDM process like, pulse time, discharge current, pause time, discharge voltage, workpiece material properties, convection and conduction heat transfer. The MRR and R_m values obtained from the developed model are compared with the experimental values taken from the literature.

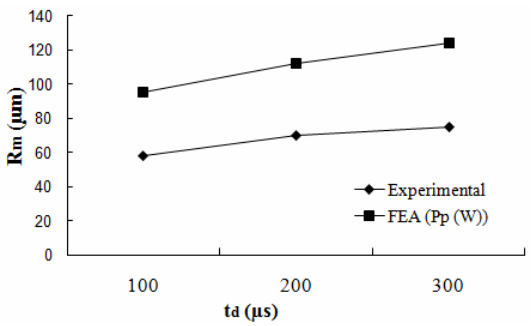

Fig. 12. Experimental [6] and FEA R_m results (P_p input to FEA).

In this study, closer theoretical results with the experimental ones given in Ref. [1] are obtained when plasma power (P_p) is input to the model. Especially for high energy pulses (i.e. with high discharge current (I_d) and long pulse time (t_d)) theoretical R_m values are found considerably lower than the experimental ones when T_p is input to the model. For machining parameter settings of $I_d < 20$ A and $t_d < 50$ µs, theoretical R_m and MRR findings from the model and the experimental results given ref [2] are consistent when the T_p is input to the model. Very consistent R_m values were obtained for 3000°C T_p. Closer R_m values with experimental results given in Ref. [6] is observed for 5000°C T_p input. It is also found that high T_p values (above 8000°C) do not give consistent R_m values with the experimental values reported in literature.

The developed model is in good agreement with the experimental R_m and MRR values reported in the literature and capable of providing good estimates for the temperature distributions, final crater shapes and removal rates in EDM. In future, the proportion of metal removed from the molten crater at different machining conditions can be determined experimentally and introduced to the model for better prediction of the actual metal removal rate especially for high energy pulse settings.

References

[1] A. Ozgedik and C. Cogun, An experimental investigation on tool wear in electric discharge machining, *Int. Journal of Advanced Manufacturing Technology*, 27 (2006) 488-500.

[2] D. D. DiBitonto, P. T. Eubank, M. R. Patel and M. A. Barrufet, Theoretical models of the electrical discharge machining process. I. A simple cathode erosion model, *J. Appl. Phys.*, 66 (9) (1989) 4095-4103.

[3] M. R. Patel, M. A. Barrufet, P. T. Eubank and D. D. DiBitonto, Theoretical models of the electrical discharge machining process. II. The anode erosion model, *J. Appl. Phys.*, 66 (9) (1989) 4104-4111.

[4] P. T. Eubank, M. R. Patel, M. A. Barrufet and B. Bozkurt, Theoretical models of the electrical discharge machining

process III.The variable mass cylindrical plasma model, *J. Appl. Phys.,*73 (11) (1993) 7900-7909.

[5] J. Marafona and J. A. G. Chousal, A finite element model of EDM based on the Joule effect, *Int. Journal of Machine Tools & Manufacture,* 46 (2006) 595-602.

[6] H. K. Kansal, S. Singh and P. Kumar, Numerical simulation of powder mixed electric discharge machining using finite element method, *Mathematical and Computer Modelling* (10) (2007) 1-21.

[7] S. Das, M. Klotz and F. Klocke, EDM simulation: finite element-based calculation of deformation, microstructure and residual stresses, *Journal of Materials Processing Technology,* 142 (2003) 434-451.

[8] V. Yadav, V. K. Jain and P. M. Dixit, Thermal stresses due to electrical discharge machining, *Int. Journal of Machine Tools & Manufacture,* 42 (2002) 877-888.

[9] R. Snoeys and F. Van Dijck, Investigations of EDM operations by means of thermo mathematical model, *Annals of CIRP,* 20 (1) (1971) 35.

[10] N. B. Salah, F. Ghanem and K. B. Atig, Numerical study of thermal aspects of electric discharge machining process, *Int. Journal of Machine Tools & Manufacture,* 46 (2006) 908-911.

[11] P. D. Kumar, Study of thermal stresses induced surface damage under growing plasma channel in electro-discharge machining, *Journal of Materials Processing Technology,* 202 (2008) 86-95.

[12] A. Singh and A. Ghosh, A thermo-electric model of material removal during electric discharge machining, *Int. Journal of Machine Tools & Manufacture*, 39 (1999) 669-682.

[13] P. Allen and X. Chen, Process simulation of micro electro-discharge machining on molybdenum, *Journal of Materials Processing Technology,* 186 (2007) 346-355.

[14] P. D. Kumar and R. K. Bhoi, Analysis of spark eroded crater formed under growing plasma channel in electro discharge machining, *Machining Science and Technology,* 9 (2005) 239-261.

[15] A. Erden and B. Kaftanoğlu, Heat transfer modelling of electric discharge machining, *Proc. 21 st. Int. Machine Tool and Des. Res. Conf.,* (1981) 351-359.

[16] K. Bhondwe, V. Yadava and G. Kathiresan, Finite element prediction of MRR due to electro-chemical spark machining, *Int. Journal of Machine Tools and Manufacture,* 46 (2006) 1699-1706.

[17] M. Mahardika and K. Mitsui, A new method for monitoring micro-electric discharge machining process, *Int. Journal of Machine Tools & Manufacture,* 48 (2008) 446-458.

[18] S. H. Yeo and P. C. Tan, Critical assessment and numerical comparison of electro thermal models in EDM, *Journal of Materials Processing Technology,* 203 (2008) 241-251.

[19] C. Cogun, Variation of discharge profile with discharge power in electric discharge machining, *JSME International Journal,* 32(3) (1989) 480-483.

[20] R. Snoeys and F. Van Dijck, Plasma channel diameter growth affects stock removal in EDM, *Annals of the CIRP,* 21 (1) (1972) 39-40.

[21] K. H. Ho and S. T. Newman, State art electrical discharge machining, *Int. Journal of Machine Tools & Manufacture,* 40 (2003) 1287-1300.

[22] J. Simao, H. G. Lee, D. K. Aspinwall, R. C. Dewes and E. M. Aspinwall, Workpiece surface modification using electrical discharge machining, *Int. Journal of Machine Tools & Manufacture,* 43 (2003) 121-128.

[23] T. Ikai and K. Hashigushi, Heat input for crater formation in EDM, *Proc. Int. Symp. for Electro Machining - ISEM XI,* EPFL, Lausanne, Switzerland, (1995) 163-170.

[24] C. Cogun, A technique and its application for evaluation of materials contributions in electric discharge machining", *Int. Journal of Machine Tool and Manufacture,* 30 (2) (1990) 19-31.

Yasin Sarikavak is a researcher at Turkish State Railways. He received B.S. and M.S. degrees in Mechanical Engineering Department of Gazi University in Ankara, Turkey. His research interests are nontraditional machining and non destructive inspection of materials.

Can Cogun is a Professor Dr. at Middle East Technical University (METU) Mechanical Engineering Department in Ankara, Turkey. His research interests are nontraditional machining, machining theory, conventional machine tools, manufacturing systems and manufacturing automation.